

Liquid-Metal-Based Stretchable Triboelectric Nanogenerators for Flowing-Liquid-Based Energy Harvesting and Self-Powered Sensor Applications

Karthikeyan Munirathinam, Gajula Prasad, Dong Su Kim, Jongsung Park,* and Dong-Weon Lee*

In this paper, a liquid-metal-based triboelectric nanogenerator (LM-TENG) is proposed for harvesting energy from flowing water and self-powered flow sensor applications. The proposed LM-TENG mainly consists of a Galinstan working electrode that is encapsulated in a polydimethylsiloxane friction layer. The triboelectric performance of the LM-TENG is optimized as a function of flow rate and frictional layer thickness. The output performance of the optimized LM-TENG (6.2 V and 3.6 μA) is superior to that of the copper-electrode-based TENG (C-TENG, 2.4 V and 0.8 μA) at the flow rate of 2.5 L min⁻¹. This is because the stretchability of the optimized LM-TENG is three times higher than that of the C-TENG, which increases the contact area and enhances the output performance. The optimized LM-TENG is successfully demonstrated as a self-powered flow sensor for remote monitoring of water flow in pipelines. In addition, the LM-TENG is capable of powering more than 30 LEDs and directly powering low-power electronics (LCDs).

flowing liquids.^[6] Among them, triboelectric nanogenerators (TENGs) have attracted attention owing to their easy integration with ambient surroundings, low cost, and high energy-conversion efficiency.^[7–12] Generally, TENGs operate based on the conjunction of contact electrification and electrostatic induction^[13–15] Most of the TENGs fabricated using solid electrode materials such as copper, gold, and aluminum harvest electrostatic energy from the environment.^[16–18] However, these solid-electrode-based TENGs can corrode, especially in flow environments involving fluid-phase chemicals, which can reduce their durability. Moreover, the properties of solid materials such as high hardness, low flexibility, and rigidity restrict their potential applications because large strains can cause

1. Introduction

Recently, piezoelectric,^[1] electrokinetic,^[2,3] and triboelectric^[4,5] nanogenerators have been developed to harvest energy from

crack development on the electrode surface during continuous operation.^[19,20] To avoid this, liquid metal electrodes have been investigated in recent TENGs for harvesting energy from the environment owing to their outstanding properties such as favorable flexibility, high durability, and avoidance of cracks and corrosion.^[21,22]

The energy transduction mechanism of TENGs depends primarily on friction between a pair of materials with opposing tribo-polarities.^[23,24] Over the years, many solid–solid friction-based TENGs have been reported.^[25,26] However, their performances are governed by the roughness of both contact surfaces, which reduces the effective contact area, especially at the nanoscale.^[27] Moreover, the friction between solid–solid contact surfaces cause power dissipation through heat, which drastically reduces the efficiency of TENGs. Therefore, in recent years, many researchers have been attracted to the concept of solid–liquid friction-based TENGs because of their advantages such as large contact area, high contact intimacy, and low friction coefficient.^[28]


Several solid–liquid friction-based TENGs have been reported, including ionic-liquid-based microfluidic nanogenerators^[29] and rainwater-based energy harvesting TENGs.^[11,30–32] Among them, rainwater is a promising candidate as the friction layer in solid–liquid-based TENGs owing to the triboelectric charges generated by contact friction with air/dielectric material.^[33–36] However, rainwater is an intermittent source and

K. Munirathinam, G. Prasad, D. S. Kim, D. Lee
MEMS and Nanotechnology Laboratory
School of Mechanical System Engineering
Chonnam National University
Gwangju 61186, Republic of Korea
E-mail: mems@jnu.ac.kr

D. S. Kim, D. Lee
Advanced Medical Device Research Center for Cardiovascular Disease
Chonnam National University
Gwangju 61186, Republic of Korea

J. Park
Department of Precision Mechanical Engineering
Kyungpook National University
Sangju 37224, Republic of Korea
E-mail: jpark40@knu.ac.kr

D. Lee
Center for Next-generation Sensor Research and Development
Chonnam National University
Gwangju 61186, Republic of Korea

 The ORCID identification number(s) for the author(s) of this article can be found under <https://doi.org/10.1002/admt.202201902>.

DOI: 10.1002/admt.202201902

is affected by seasonal and geometrical dependency; therefore, power generation would not be possible under dry conditions. By contrast, it is viable to use flowing water for power generation. In this context, the water flowing through pipelines and channels seems the most accessible energy source. In recent years, a few studies on harvesting energy from flowing water have been conducted.^[37,38] However, the technologies to convert the energy present in flowing water have rarely been investigated as self-powered flow sensors in pipelines and microchannel. For instance, Cui et al.^[38] reported a solid electrode tube based TENG as a self-powered sensor for monitoring water flow and blockage in pipelines. The authors used several electrodes in the tube to detect water position, flow rate, and blockage in the pipeline. The PTFE and copper based tubular nanogenerator was proposed for self-powered medical device.^[37] Though the authors successfully demonstrated tube-based TENG for self-powered sensor applications, the use of solid electrodes in TENG could cause corrosion, especially in low-flow rate-based chemical environments. Furthermore, as the microchannel and pipelines in remote locations are dedicated to continuous operation, solid electrodes can develop cracks easily during their continuous operation. Thus, the liquid-metal electrode-based TENG could help in building a robust and reliable self-powered sensor for monitoring liquid flows in microchannel and pipelines. To the best of our knowledge, a liquid-metal-based TENG for harvesting energy from flowing water has not been explored yet, and credit more investigation into self-powered flow sensor applications.

Herein, we demonstrate a liquid-metal-based triboelectric nanogenerator (LM-TENG) for harvesting energy from flowing water and a self-powered flow sensor for monitoring pipelines, as shown in **Figure 1**. The proposed LM-TENG consists of a liquid metal Galinstan electrode encapsulated in a polydimethylsiloxane (PDMS) thin-film friction layer. The energy transduction mechanism of the LM-TENG depends primarily on the friction between the solid and liquid (PDMS–water) surfaces. The performance of the LM-TENG (6.2 V and 3.6 μ A) is superior to that of the copper-electrode-based TENG (C-TENG 2.4 V and 0.8 μ A) owing to the higher stretchability of the liquid

metal electrode. Furthermore, a vertical LM-TENG is placed perpendicular to the direction of water flow to demonstrate its application as a self-powered flow sensor. This sensor is used to monitor the flow rate of water in a remote environment, and it indicates different flow rates by glowing commercial LEDs. Finally, a horizontal LM-TENG for monitoring the flow of liquid in a microchannel is tested as a self-powered flow sensor that can directly power a liquid crystal display.

2. Results and Discussions

The key steps in the fabrication of the LM-TENG and C-TENG are shown in **Figure 2**. Initially, a PDMS layer with a microchannel was prepared by a lithography process. The detailed fabrication process is illustrated in Experimental Section. For achieving an LM-TENG, liquid-metal Galinstan was injected into the PDMS microchannel, while a double-sided adhesive conductive copper tape was pasted in the PDMS microchannel to form C-TENG (Figure 2ai–vii). Next, a horizontal LM-TENG (Figure 2b) fabricated by sandwiching two LM-TENGs between a microchannel was used to demonstrate self-power flow sensor application in water pipelines. Furthermore, a vertical LM-TENG (Figure 2c) was fabricated by fixing LM-TENGs perpendicular to the direction of liquid flow for self-power flow sensor application in microchannels. Two types of water were used to evaluate the characteristics of the TENGs fabricated herein. Tap water flowing from a household faucet was used as the source for the vertical LM-TENG structure, and water injected continuously through a hollow space by using a syringe pump was used as the source for the horizontal LM-TENG.

The working mechanism of an LM-TENG is based on the triboelectrification process that occurs between the PDMS and the flowing water. The LM-TENG consists of a Galinstan electrode encapsulated in a PDMS microchannel, which acts as the friction layer, while the flowing water acts as the sliding layer. The contact electrification process between the flowing water and the air/insulating pipe creates triboelectric charges in the water during its flow. As reported in literature^[11], when

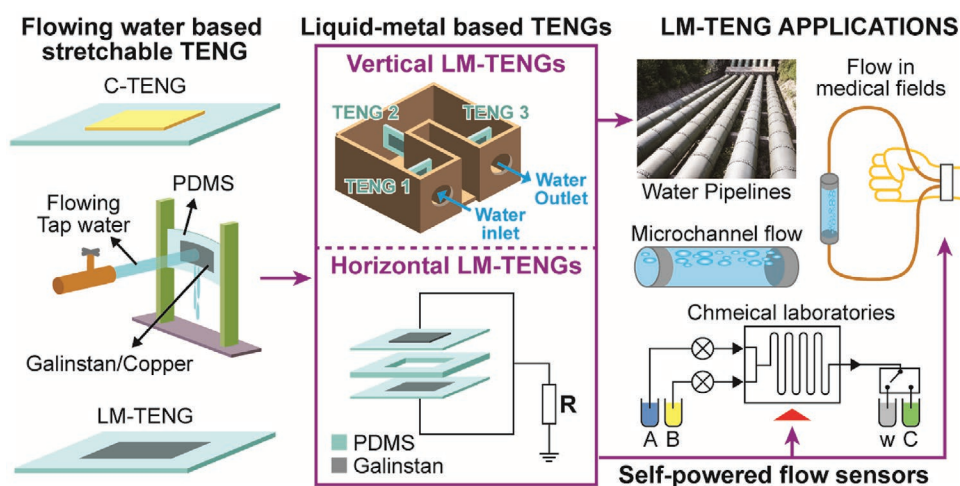


Figure 1. Schematic representation of stretchable triboelectric nanogenerator (TENG) for water energy harvesting and self-powered flow sensor applications.

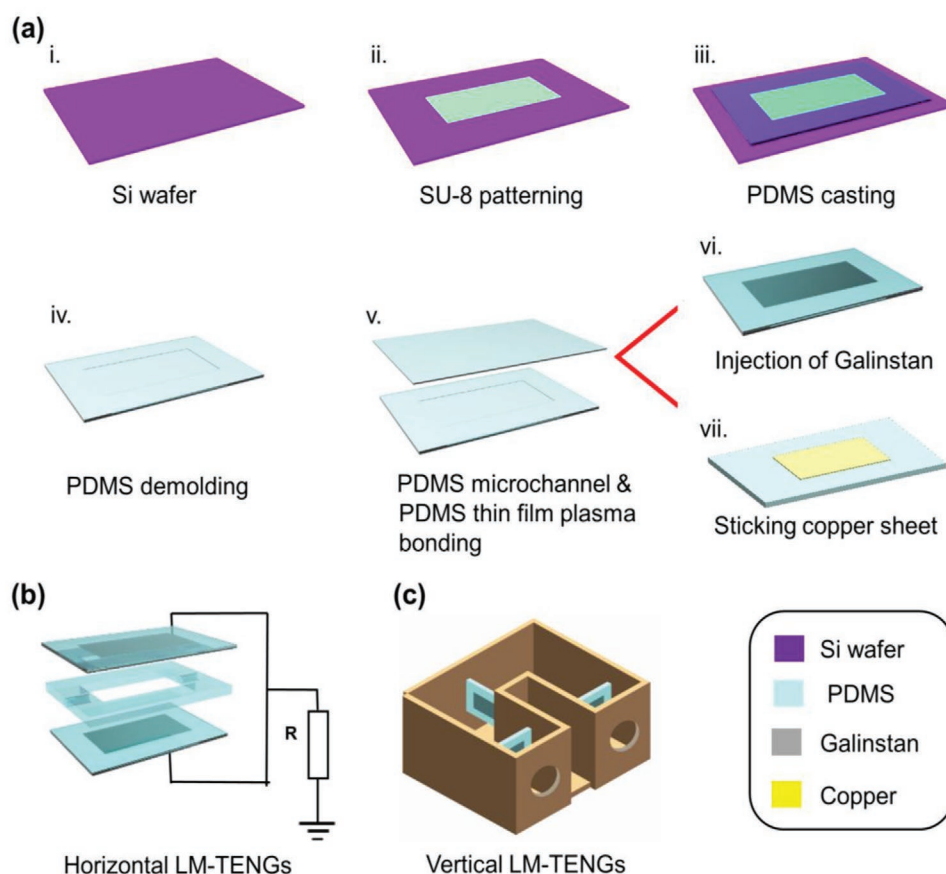


Figure 2. Schematic diagram of proposed triboelectric nanogenerator (TENG). ai–vii) Fabrication process flow of liquid-metal-based TENG (LM-TENG) and copper-electrode-based TENG (C-TENG). LM-TENGs placed horizontal (b) and vertical (c) to the direction of liquid flow for harvesting energy from a microchannel and a pipeline, respectively.

the water contacts the PDMS layer, the PDMS surface becomes negatively charged via contact electrification. This negatively charged PDMS layer attracts H^+ ions present in the water and forms an electrical double layer (EDL). The EDL consists of three layers, namely the Inner Helmholtz Plane (IHP), Outer Helmholtz Plane (OHP), and bulk phase (Figure 3a). When the water flows, the transportation direction of H^+ ions in the EDL is influenced by the electrostatic attraction force. In the IHP, the H^+ ions move tangentially along the direction of water flow over the PDMS surface due to its strong electrostatic attraction force. On the other hand, the counter ions exist together with the H^+ ions in the OHP.^[29] Additionally, the negatively charged OH^- ions in the OHP move toward the bulk phase due to weak electrostatic attraction force. As a result, once the water flows, the charge neutrality in the EDL is disrupted and develops an electrostatic potential difference between the PDMS and water interface, resulting in the generation of AC waveform at the output.

The generation of AC waveform is explained based on the sequential contact-electrification and electrostatic induction process of water entering and leaving the device, as reported by Lin et al.^[11] and Munirathinam et al.^[37] Herein, water from a household faucet is continuously passed into the LM-TENG. Once the water comes into contact with the PDMS layer, a positive potential difference is established between the Galinstan

electrode and the ground electrode, as shown in (Figure 3bi). As the water flow and aligns the Galinstan electrode, electrons flow from the ground to the electrode, as shown in Figure 3bii. This electron flows until the potential difference becomes zero and an equilibrium is reached, as shown in Figure 3biii. When the water droplets leave the PDMS surface, the direction of the current is reversed, and the electrons flow from the Galinstan electrode to the ground, as shown in Figure 3biv, until a new equilibrium is reached (Figure 3bv). Thus, the flowing water, with initial triboelectric charges, can cause electrons to flow between the electrode and the ground and produce a negative and positive component of the AC signal, as shown in Figure 3c.

To optimize the TENG parameters for harvesting energy from flowing water, a stretchability test was conducted on the C-TENG and LM-TENG, as shown in Figure 4. Here, the LM-TENG and C-TENG with an initial length of 29 mm were fixed using a supporting structure, as illustrated in Figure 4a. The elongations of the C-TENG and LM-TENG due to water flowing at a rate of $0\text{--}2.5\text{ L min}^{-1}$ were measured, as shown in Movie S1 (Supporting Information). The maximum elongations of the C-TENG and LM-TENG were 2 and 6 mm, respectively (Figure 4b). The corresponding increases in length are shown in Figure S1 (Supporting Information). Here, the percentage elongation L_x is defined as follows:

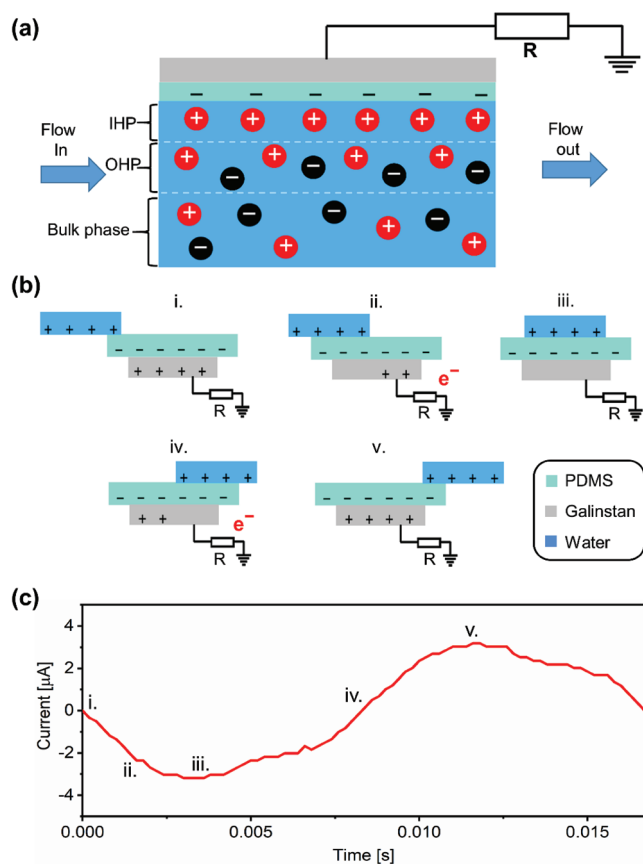


Figure 3. a) Schematic illustrations of working principle of the liquid-metal-based triboelectric nanogenerator (LM-TENG) based on electrical double layer (EDL) model. b) Energy harvesting mechanism based on the continuous entry and exit of flowing water. c) Alternating current waveform generated by the flowing water.

$$Lx(\%) = \frac{(L - L_0)}{L} \times 100 \quad (1)$$

where L_0 is the initial electrode length, and L is the electrode length after it is stretched by the flowing water. As calculated in Figure S2 (Supporting Information) and shown in Figure 4c, the lengths of the C-TENG and LM-TENG electrodes increased by 7% and 20%, respectively. The electrical outputs of the C-TENG and LM-TENG were compared at different flow rates (Figure 4d,e and Figures S3 and S4, Supporting Information). Owing to the low Young's modulus of Galinstan, the LM-TENG electrode stretched considerably and produced a maximum output voltage of 6.2 V and current of 3.6 μA (Figure S3, Supporting Information) at a flow rate of 2.5 L min^{-1} , while the performance of the C-TENG was relatively weak. This result can be explained on the basis of the combined effect of PDMS thickness and electrode resistance. According to the Poisson effect, when the PDMS is stretched, its thickness decreases, and the number of induced charges into the Galinstan electrode increases.^[21] Similarly, when a PDMS film is stretched, the resistance of the liquid-metal electrode increases. However, owing to the high-impedance nature of LM-TENGs, the change in resistance is negligible compared to the output. Moreover, the performance of the LM-TENG depends largely on the

thickness of the PDMS friction layer. The electrical output of the LM-TENG decreases as the PDMS layer thickness increases, as shown in Figure 4f and Figure S5 (Supporting Information). This result is attributed to the fact that the triboelectric charges present in water are induced into the Galinstan electrode owing to the electrostatic force of the flowing water. Because the electrostatic force is inversely proportional to the distance (PDMS thickness) between the tribo-charges and the Galinstan electrode, a high PDMS film thickness reduces the electrostatic force acting on the Galinstan electrode, which reduces the number of electrostatically induced charges at the electrode. Conversely, a low PDMS thickness increases the electrostatic force acting on the electrode, thus increasing the number of electrostatically induced charges at the electrode. This behavior shows strong evidence of contact electrification at the PDMS–water contact surface and validates the working mechanism of the LM-TENG. Thus, the LM-TENG emerges as the obvious choice for harvesting energy from flowing water.

To investigate the electrical output of the optimized LM-TENG, tap water was allowed to continuously impinge upon the device at a flow rate of 2.5 L min^{-1} . The horizontal impinging distance between the water outlet of the faucet and the LM-TENG was approximately 25 mm. The real-time voltage and current waveforms of the device are shown in Figure 5a,b. For the LM-TENG with the optimized PDMS film thickness of 200 μm , the total voltage and current per cycle reached 6.2 V and 3.6 μA , respectively. Because the flow of water from the faucet was not a controlled flow, the output waveforms exhibited fluctuations. Moreover, the electrical output of the LM-TENG was investigated by connecting different resistance loads to it, as shown in Figure 5c. When the resistance load was approximately 0.1 $\text{M}\Omega$, the voltage was close to 0, and the current did not change significantly. When the load resistance was increased from 0.1 to 20 $\text{M}\Omega$, the voltage through the load increased, but the current across the load tended to decrease. Therefore, the instantaneous power density across the load remained small when the resistance was low and reached a maximum of 0.32 W m^{-2} at 10 $\text{M}\Omega$, as shown in Figure 5d. Finally, the reliability and consistency of power generation in accordance with material degradation when exposed to continuous water flow was investigated over a period of time. The power generation of LM-TENG for water flowing at 2.5 L min^{-1} was recorded on 15 individual days, as shown in Figure 5e. It can be observed that the output performance of LM-TENG did not degrade significantly even after 15 days, indicating its outstanding device reliability and consistency. Further, the continuous operation of LM-TENG for 1 h (Figure 5e inset) displays that the output voltage is comparable on days 1 and 15, confirming the stability and reproducibility of the device.

The applications of LM-TENGs as self-powered flow sensors were evaluated using vertical and horizontal LM-TENGs. The proposed LM-TENG can generate a continuous electrical signal from flowing water, indicating its potential for use as a self-powered sensor in water flow environments. Water flows through many pipeline systems, especially through long-distance water transport and large-diameter pipelines. Accordingly, it is important to monitor the fluid flow parameters (flow rate) in large-diameter pipelines. Similarly, the use of

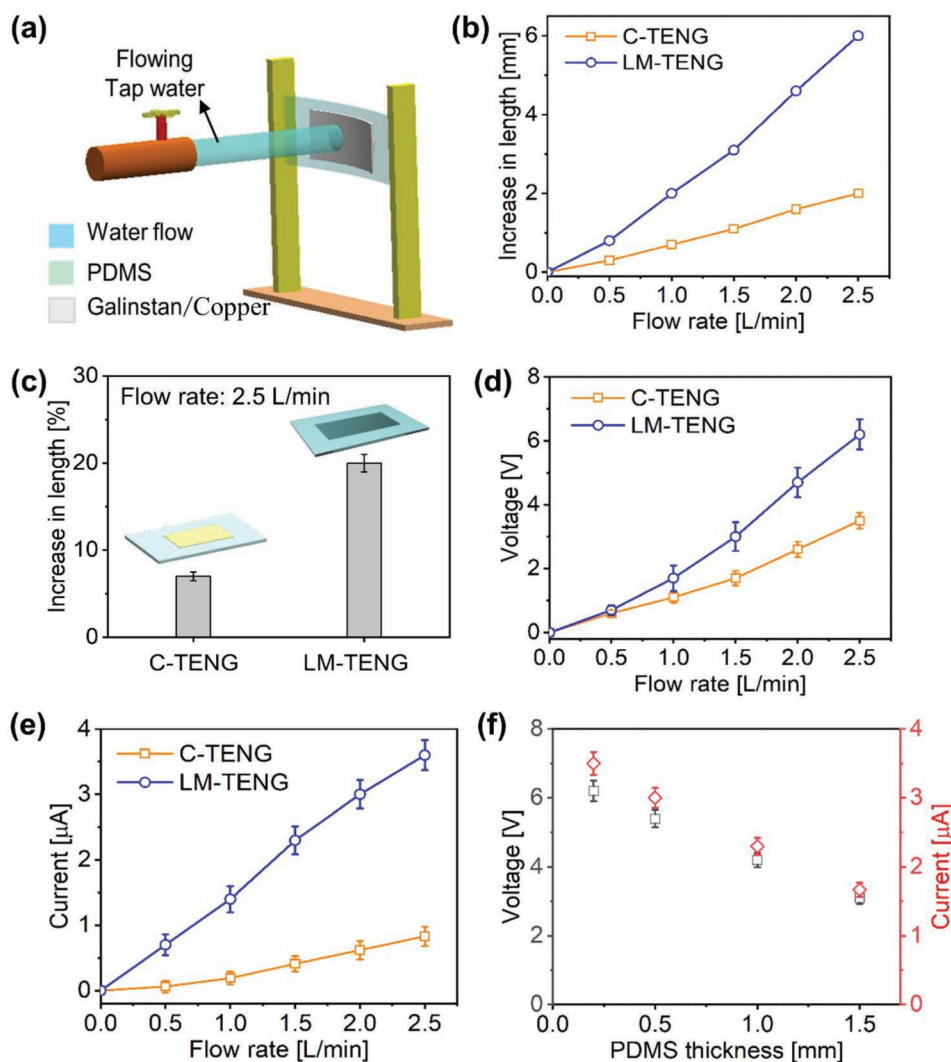


Figure 4. a) Schematic illustration of stretchability measurement of copper-electrode-based triboelectric nanogenerator (C-TENG) (polydimethylsiloxane (PDMS) + copper) and liquid-metal-based TENG (LM-TENG) (PDMS + Galinstan) fixed at both ends on a supporting stand. b,c) The increase in length and percentage of increase in length of the device under various flow rates. d,e) Voltage and current output performance of LM-TENG and C-TENG as a function of the flow rate. f) Effect of PDMS layer thickness on LM-TENG performance.

fluid flow in small-sized tubing or channels has increased rapidly in multidisciplinary fields such as chemical, medical, and lab-on-chip. In such applications, because fluids flow at low rates, any flow stoppage can cause chemical mishaps, especially in chemical and medical laboratories. Consequently, technologies for monitoring fluid flows with low flow rates have attracted considerable attention. Several techniques have been reported for monitoring the fluid flows through small channels by using solid electrodes. However, the chemical and medical environments with low flow rates and prolonged continuous operation can cause corrosion and cracking of the electrodes, thereby reducing the durability of the solid electrode-based sensors. Therefore, sensors with simple structures and self-powering capability are strongly preferred for developing water flow monitoring systems in water pipelines and microchannel.

Initially, a self-powered flow sensor was demonstrated for monitoring flow rate in water pipelines, by using a vertical

LM-TENG placed perpendicular to the direction of water flow was used, as shown in **Figure 6**. Herein, three vertical LM-TENGs (TENG 1, TENG 2, and TENG 3) were placed such that the distance between the two LM-TENGs were 8 cm, as shown in Figure 6a. Regulated tap water was allowed to flow into the LM-TENGs. Figure 6b shows the voltage and current outputs obtained by increasing the number of vertical LM-TENGs while maintaining a constant water flow rate of 2.5 L min⁻¹. As the water flow rate was varied from 0.5 to 2.5 L min⁻¹, the maximum output voltage and current of the vertical LM-TENG array were 11 V and 6.2 μA respectively, as shown in Figure 6c. The outputs of the individual vertical LM-TENGs were added using a bread board and then rectified to power the LEDs, as shown in Figure 6d. The various flow rates of tap water (0.5, 1.5, and 2.5 L min⁻¹) were distinguished by glowing different numbers of LEDs (11, 20, and 31), as shown in Figure 6e and Movie S2 (Supporting Information). Although the monitoring

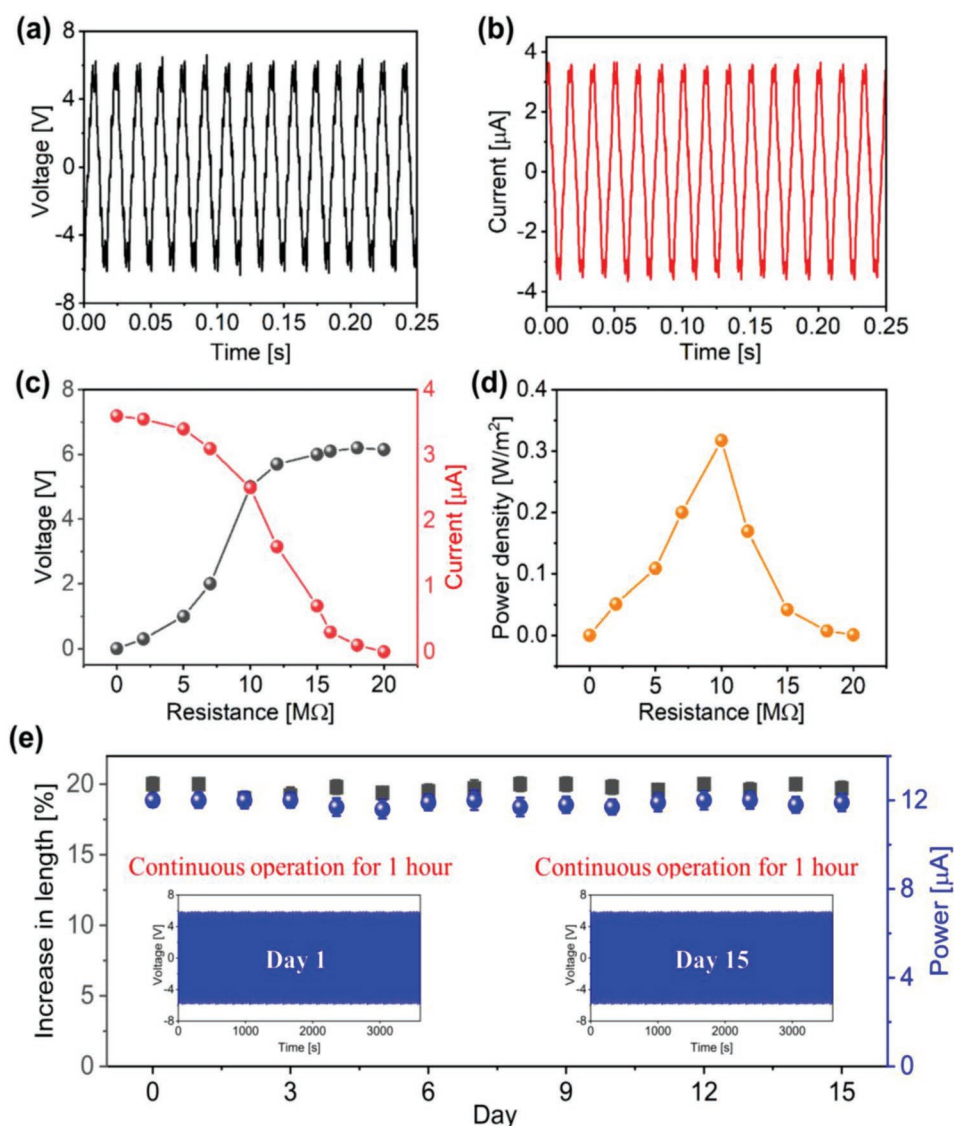


Figure 5. Electrical performance of liquid-metal-based triboelectric nanogenerator (LM-TENG) for tap water flowing at 2.5 L min^{-1} . a,b) Voltage and current waveforms. c) Triboelectric performance (voltage and current) as a function of input load resistance. d) Power density. e) Material degradation and stability test of LM-TENG for up to 15 days. (Inset (e): continuous operation for 1 h on day 1 and day 15).

of water flow rate was demonstrated using the vertical LM-TENGs placed perpendicular to the water flow direction, the self-powered sensor is expected to not significantly affect the change in water flow rate especially in larger-diameter pipelines.

Next, we demonstrate a horizontal LM-TENG as a self-powered flow sensor for monitoring the flow of liquid through channels at low flow rates. The horizontal LM-TENG structure is composed of a Galinstan electrode, 200- μm -thick PDMS friction layer, and a microchannel for liquid flow as shown in **Figure 7a**. The electrical performance of LM-TENG, compared with different microchannel widths (0.5, 1, 1.5, and 2 mm), is shown in Figure S6 (Supporting Information). The experimental data shows that the output voltage and current have no significant difference. However, an LM-TENG, with a 2 mm width microchannel, was selected for convenient

fabrication. Hence the LM-TENG with 2 mm microchannel width was selected for further characterizations. The horizontal LM-TENG uses flowing liquid as the energy source for the energy-harvesting and sensor applications. Initially, the TENGs were used to distinguish different liquid environments in the channel. For instance, different liquid solutions were continuously passed into the horizontal LM-TENG at a flow rate of 1 mL min^{-1} by using a 30 mm diameter syringe attached to the syringe pump, as shown in **Figure 7b**. The electrical outputs of the horizontal LM-TENG were measured for different liquids, as shown in **Figure 7c**. The output performance of the horizontal LM-TENG for tap water was higher than those for DI water, and ethanol because of their lower conductivities. This is because the tap water contained more dissolved salts, which led to a higher output, whereas the ethanol produced the least output because it did not contain any dissolved salts. These

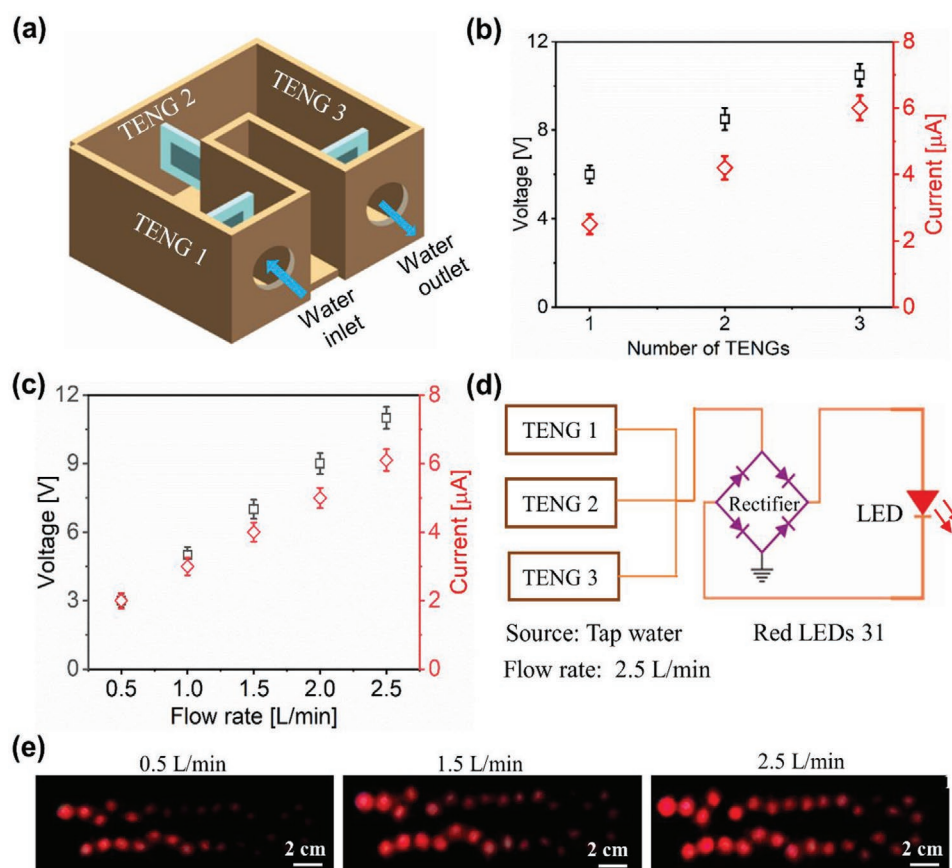


Figure 6. Demonstration of vertical liquid-metal-based triboelectric nanogenerator (LM-TENG) as a self-powered flow sensor. a) Cross-sectional view of the vertical TENG. b) Voltage and current outputs of vertical LM-TENGs under a tap water flow of 2.5 L min^{-1} . c) Voltage and current outputs of the three vertical LM-TENGs as a function of water flow rate. d) Circuit diagram for lighting up LEDs. e) Flow rate indication by lighting up different numbers of LEDs.

results indicate that the horizontal TENG can be used as a self-powered sensor to monitor various liquids flowing through a microchannel. Furthermore, the horizontal LM-TENG was used to monitor different ionic liquids. Three kinds of ionic solutions, KOH, KCl, and NaCl, with 1 M concentration were tested, as shown in Figure S7 (Supporting Information). The electrical output of KOH was higher than those of KCl and NaCl. This is because the electrical conductivity of KOH (1.5 S m^{-1}) is higher than that of other ionic solutions. Similarly, the electrical output of KCl is higher than NaCl due to the high electrical conductivity of KCl (1.29 S m^{-1}) compared to NaCl's (1.15 S m^{-1}). The ionic liquids flowing through the microchannel can be identified based on the electrical output. Thus, the LM-TENG can monitor different liquids flowing through the microchannel at low flow rates.

Additionally, the horizontal LM-TENG was tested to monitor liquid flow using tap water. Tap water was passed continuously into the horizontal LM-TENG at a flow rate of 1 mL min^{-1} . Figure 7d,e shows the maximum output voltage and current of the horizontal LM-TENG. When the water valve was turned on, the continuous flow of water generated a constant voltage and current of 2.02 V and $0.6 \mu\text{A}$, respectively. When the water valve was turned off, the voltage and current generated by the horizontal LM-TENG decreased immediately. A commercially

available LCD was used to display the water flow inside the microchannel. The horizontal LM-TENG was connected directly to the LCD, as shown in Figure 7f. As soon as water started to flow through the horizontal LM-TENG, the LCD started to glow continuously (ON state) until the water flowed. Once the water flow was stopped (OFF state), the LCD did not glow. This setup can be implemented easily in chemical and medical environments for monitoring fluid flows. The horizontal-LM-TENG-based self-powered flow sensor for monitoring the flow of liquid in a microchannel is shown in Movie S3 (Supporting Information).

3. Conclusions

In summary, we developed a liquid-metal-based triboelectric nanogenerator (LM-TENG) for harvesting energy from flowing water and monitoring the flow of liquids in remote environments. The LM-TENG consisted of a liquid-metal Galinstan electrode encapsulated in a $200\text{-}\mu\text{m}$ -thick PDMS thin-film friction layer. The performance of the LM-TENG was superior to that of the C-TENG owing to the higher stretchability of the liquid-metal electrode. The excellent liquid property of Galinstan ensures that the LM-TENG is stretchable under

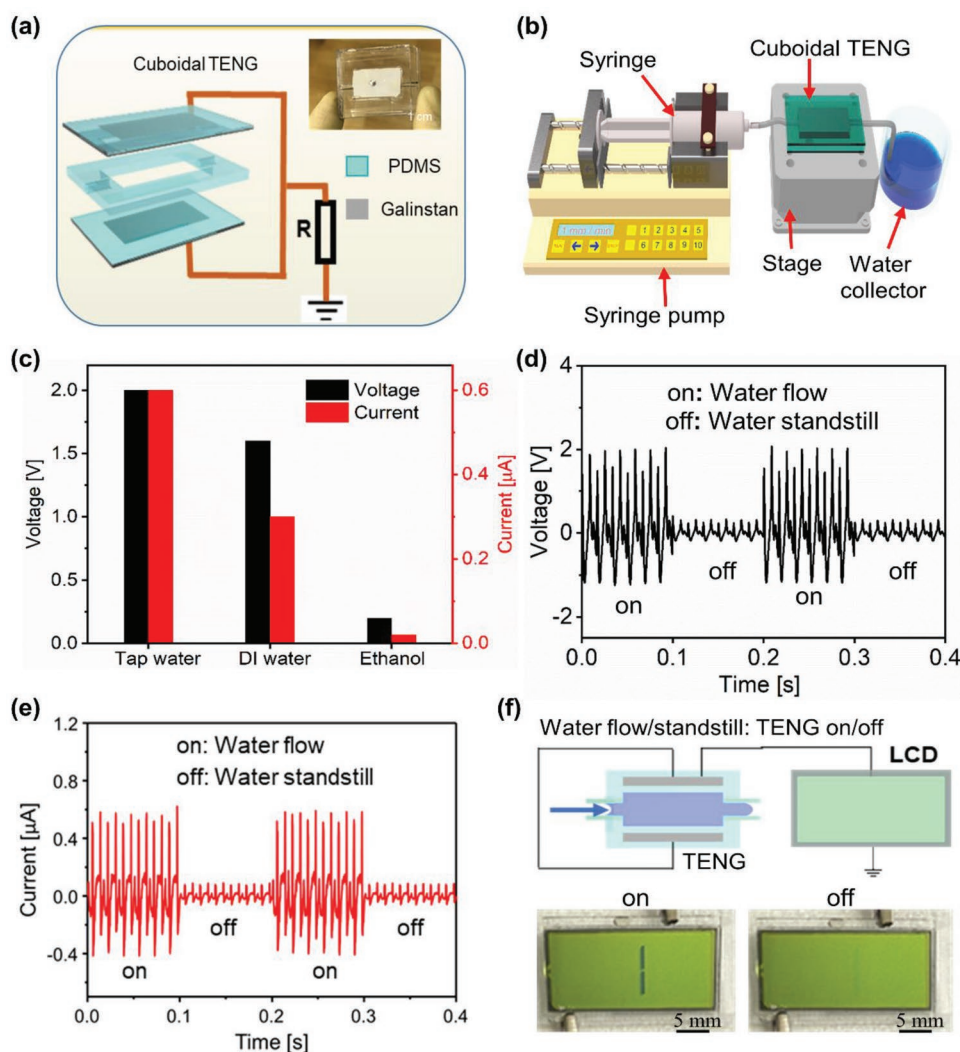


Figure 7. Characterization of horizontal liquid-metal-based triboelectric nanogenerator (LM-TENG) as a self-powered flow sensor. a) Schematic of horizontal LM-TENG. b) Experimental set up for a liquid flow rate of 1 mL min^{-1} . c) Performance of horizontal LM-TENG as a self-powered liquid sensor. d,e) Voltage and current measurements of water flow in the on and off states. f) Electrical circuit and images of the LCD indicating the on and off states of the flowing water.

a mechanical force and enhances its output performance. A vertical LM-TENG consisting of three individual LM-TENGs was demonstrated as self-powered flow sensor that powers different numbers of commercial LEDs to correspond to different flow rates. In addition, a horizontal LM-TENG was demonstrated as a self-powered flow sensor for monitoring liquid flows through microchannels. In sum, the results of this work are promising and can drive the development of liquid-metal-based TENGs for harvesting energy from flowing water and self-powered liquid flow monitoring systems at remote locations.

4. Experimental Section

Fabrication of the LM-TENG and C-TENG: First, an SU-8 (3010) pattern with a length of 23 mm, a width of 10 mm, and a thickness of 40 μm was fabricated on a four-inch silicon wafer by using lithography

(Figure 2ai,ii). Then, a PDMS solution was prepared by mixing the base elastomer (Sylgard 184, Dow Corning Corp., Auburn, MI, USA) with a curing agent in a ratio of 10:1. After degassing, the solution was spin-coated at 500 rpm on the silicon wafer in a 40-μm mold and allowed to cure on a hot plate at 80°C for 2 h (Figure 2aiii). Thereafter, the PDMS layer with 200-μm -thick, 29 mm length, and 40-μm microchannel was carefully peeled off from the wafer, as depicted in Figure 2aiv. In the next step, a 200-μm -thick PDMS top layer was prepared by spin-coating PDMS on the silicon wafer and curing it at 80°C for 2 h. For fabricating the LM-TENG, the PDMS layer with the microchannel and the top PDMS layer were bonded together by following a low-pressure oxygen plasma bonding process at 100 W for 60 s (Figure 2av). After plasma bonding, the attached PDMS layers were heated on a hot plate at 80°C for 1 h to improve the interlayer chemical bonding. Subsequently, the liquid metal Galinstan (Gallium Indium Tin Alloy, Ga: 68.5% In: 21.5% Sn: 10%, Electrical conductivity: $3.46 \times 10^6 \text{ S m}^{-1}$, Purity: 99.9%) was injected into the PDMS microchannel by using a syringe pump at a flow rate of 0.2 mL min^{-1} (Figure 2avi). Furthermore, the PDMS friction layer of the LM-TENG was fabricated with different thicknesses by bonding 100- and 200-μm -thick layers in different combinations. To achieve thicknesses of 0.5, 1, and 1.5 mm, two 200-μm -thick and one 100-μm -thick layers, five

200-mm-thick layers, seven 200-mm-thick, and one 100-mm-thick layers, respectively, were bonded using a low-pressure oxygen plasma bonding process. For fabricating the C-TENG, a double-sided adhesive conductive copper tape was pasted in the PDMS microchannel and encapsulated in a PDMS top layer, as shown in Figure 2avii. Furthermore, a horizontal LM-TENG was fabricated by sandwiching two LM-TENGs between a microchannel, while a vertical LM-TENG was fabricated by fixing LM-TENGs perpendicular to the direction of liquid flow, as shown in Figure 1b,c, respectively.

Measurements and Characterization of LM-TENG: Two types of flowing water were used to evaluate the characteristics of the two TENGs fabricated herein. Tap water flowing from a household faucet was used as the source for the vertical LM-TENG structure, and water injected continuously through a hollow space by using a syringe pump was used as the source for the horizontal LM-TENG. Additionally, various liquids (Tap water, DI water, and ethanol) were tested for the horizontal LM-TENG. The voltages and currents were measured using a Tektronix TDS 2014B oscilloscope and a low-noise current amplifier (Stanford Research Systems, SR570), respectively.

Supporting Information

Supporting Information is available from the Wiley Online Library or from the author.

Acknowledgements

This study was supported through a National Research Foundation of Korea (NRF) grant funded by the Korean government (MSIT) (No. 2020R1A5A8018367).

Conflict of Interest

The authors declare no conflict of interest.

Data Availability Statement

The data that support the findings of this study are available from the corresponding author upon reasonable request.

Keywords

flowing water, horizontal and vertical LM-TENGs, liquid-metal TENGs, self-powered flow sensors, stretchability

Received: November 9, 2022

Revised: February 15, 2023

Published online:

- [1] Y. Hu, Z. L. Wang, *Nano Energy* **2015**, *14*, 3.
- [2] A. Mansouri, S. Bhattacharjee, L. Kostiuik, *Lab Chip* **2012**, *12*, 4033.
- [3] C. L. Berli, M. L. Olivares, *J. Colloid Interface Sci.* **2008**, *320*, 582.
- [4] J. S. Kim, J. Kim, J. N. Kim, J. Ahn, J. H. Jeong, I. Park, D. Kim, I. K. Oh, *Adv. Energy Mater.* **2022**, *12*, 2103076.
- [5] Z. L. Wang, *ACS Nano* **2013**, *7*, 9533.

- [6] H. F. Liew, A. R. Rosemizi, M. F. Romli, M. T. Nuraidah, *J. Phys.: Conf. Ser.* **2021**, *1793*, 012041.
- [7] C. Wu, A. C. Wang, W. Ding, H. Guo, Z. L. Wang, *Adv. Energy Mater.* **2019**, *9*, 1802906.
- [8] Z. Wang, D. Wan, R. Fang, Z. Yuan, K. Zhuo, T. Wang, H. Zhang, *Appl. Surf. Sci.* **2022**, *605*, 154765.
- [9] Z. H. Lin, G. Cheng, W. Wu, K. C. Pradel, Z. L. Wang, *ACS Nano* **2014**, *8*, 6440.
- [10] X. Liang, S. Liu, Z. Ren, T. Jiang, Z. L. Wang, *Adv. Funct. Mater.* **2022**, *32*, 2205313.
- [11] Z. H. Lin, G. Cheng, S. Lee, K. C. Pradel, Z. L. Wang, *Adv. Mater.* **2014**, *26*, 4690.
- [12] G. Cheng, Z. H. Lin, Z. L. Du, Z. L. Wang, *ACS Nano* **2014**, *8*, 1932.
- [13] Z. L. Wang, J. Chen, L. Lin, *Energy Environ. Sci.* **2015**, *8*, 2250.
- [14] X. Wei, Z. Zhao, C. Zhang, W. Yuan, Z. Wu, J. Wang, Z. L. Wang, *ACS Nano* **2021**, *15*, 13200.
- [15] S. Niu, Y. Liu, S. Wang, L. Lin, Y. S. Zhou, Y. Hu, Z. L. Wang, *Adv. Funct. Mater.* **2014**, *24*, 3332.
- [16] D. W. Kim, J. H. Lee, J. K. Kim, U. Jeong, *NPG Asia Mater.* **2020**, *12*, 1.
- [17] G. Zhu, J. Chen, Y. Liu, P. Bai, Y. S. Zhou, Q. Jing, C. Pan, Z. L. Wang, *Nano Lett.* **2013**, *13*, 2282.
- [18] C. Zhang, L. Liu, L. Zhou, X. Yin, X. Wei, Y. Hu, Y. Liu, S. Chen, J. Wang, Z. L. Wang, *ACS Nano* **2020**, *14*, 7092.
- [19] X. Pu, M. Liu, X. Chen, J. Sun, C. Du, Y. Zhang, J. Zhai, W. Hu, Z. L. Wang, *Sci. Adv.* **2017**, *3*, 1700015.
- [20] S. Wang, L. Lin, Y. Xie, Q. Jing, S. Niu, Z. L. Wang, *Nano Lett.* **2013**, *13*, 2226.
- [21] Y. Yang, N. Sun, Z. Wen, P. Cheng, H. Zheng, H. Shao, Y. Xia, C. Chen, H. Lan, X. Xie, *ACS Nano* **2018**, *12*, 2027.
- [22] S. Wang, L. Ding, X. Fan, W. Jiang, X. Gong, *Nano Energy* **2018**, *53*, 863.
- [23] L. S. McCarty, G. M. Whitesides, *Angew. Chem., Int. Ed. Engl.* **2008**, *47*, 2188.
- [24] C. Duke, T. Fabish, *Int. J. Appl. Phys.* **1978**, *49*, 315.
- [25] W. Du, X. Han, L. Lin, M. Chen, X. Li, C. Pan, Z. L. Wang, *Adv. Energy Mater.* **2014**, *4*, 1301592.
- [26] J. Zhu, M. Zhu, Q. Shi, F. Wen, L. Liu, B. Dong, A. Haroun, Y. Yang, P. Vachon, X. Guo, T. He, *EcoMat* **2020**, *2*, e12058.
- [27] B. Meng, X. Cheng, X. Zhang, M. Han, W. Liu, H. Zhang, *Appl. Phys. Lett.* **2014**, *104*, 103904.
- [28] W. Tang, T. Jiang, F. R. Fan, A. F. Yu, C. Zhang, X. Cao, Z. L. Wang, *Adv. Funct. Mater.* **2015**, *25*, 3718.
- [29] K. Liu, t. Ding, x. Mo, Q. Chen, P. Yang, J. Li, W. Xie, Y. Zhou, J. Zhou, *Nano Energy* **2016**, *30*, 684.
- [30] L. Zheng, Z. H. Lin, G. Cheng, W. Wu, X. Wen, S. Lee, Z. L. Wang, *Nano Energy* **2014**, *9*, 291.
- [31] Y. Zeng, Y. Luo, Y. Lu, X. Cao, *Nano Energy* **2022**, *98*, 107316.
- [32] H. Liu, J. Dong, H. Zhou, X. Yang, C. Xu, Y. Yao, G. Zhou, S. Zhang, Q. Song, *ACS Appl. Electron. Mater.* **2021**, *3*, 4162.
- [33] D. Choi, H. Lee, I. S. Kang, G. Lim, D. S. Kim, K. H. Kang, *Sci. Rep.* **2013**, *3*, 2037.
- [34] K. Yatsuzuka, Y. Higashiyama, K. Asano, *IEEE Trans. Ind. Appl.* **1996**, *32*, 825.
- [35] Z. H. Lin, G. Cheng, L. Lin, S. Lee, Z. L. Wang, *Angew. Chem., Int. Ed. Engl.* **2013**, *52*, 12545.
- [36] Z. Zhu, H. Xiang, Y. Zeng, J. Zhu, X. Cao, N. Wang, Z. L. Wang, *Nano Energy* **2022**, *93*, 106776.
- [37] K. Munirathinam, D. S. Kim, A. Shanmugasundaram, J. Park, Y. J. Jeong, D. W. Lee, *Nano Energy* **2022**, *102*, 107675.
- [38] X. Cui, H. Zhang, S. Cao, Z. Yuan, J. Ding, S. Sang, *Nano Energy* **2018**, *52*, 71.